Isomeric electronic states in concentric quantum rings

José María Escartín,[1] Francesc Malet,[2] Agustí Emperador,[3] and Martí Pi[1]
[1]*Departament ECM, Facultat de Física, and IN²UB, Universitat de Barcelona, Diagonal 647, 08028 Barcelona, Spain*
[2]*Mathematical Physics, LTH, Lund University, P.O. Box 118, 22100 Lund, Sweden*
[3]*Institute for Research in Biomedicine, Parc Científic de Barcelona, Josep Samitier 1-5, 08028 Barcelona, Spain*
(Received 1 April 2009; revised manuscript received 20 May 2009; published 18 June 2009)

We show that polarized few-electron concentric double quantum rings display localized states that are the quantum analog of classical equilibrium ones. These states have very similar energies but fairly different angular momenta, constituting a new physical realization of the isomeric states found in nuclear and molecular physics. Their fingerprint is a very soft mode in the infrared-absorption spectrum at nearly the dipole excitation energy of a rigidly rotating N-electron molecule. The yrast line and the infrared-absorption spectrum are discussed for $N=4$ and 6 electron configurations.

DOI: 10.1103/PhysRevB.79.245317 PACS number(s): 73.21.La, 73.22.−f, 78.67.Hc

I. INTRODUCTION

It is theoretically well established that confined fermions or bosons may form localized many-particle states that bear some properties of ordinary molecules.[1–3] These molecular states, arising from strong correlations between repulsively interacting particles, are often called Wigner molecules, and their appearance is a most natural example of a spontaneous symmetry breaking (see Ref. 3 for a comprehensive discussion).

Quasi-two-dimensional semiconductor heterostructures, such as quantum dots and quantum rings, are systems especially well suited to address localized many-electron states. They can be arranged into fairly dilute systems, which favor localization, and can be submitted to magnetic fields of up to several tens of teslas that, due to the small effective mass of the confined electrons and the large dielectric constant of the material, cause the same effect that only magnetic fields in the 10^5 T range may produce on the atomic electron cloud. Examples of such electron localization can be found, e.g., in Refs. 2–4 for quantum dots and quantum dot molecules.

The nonsimply connected topology of quantum rings makes these nanostructures particularly appealing. Several works have shown that under certain circumstances electrons are azimuthally localized within the ring.[2,5] In this work we show that a similar localization, accompanied by a radial one, can be achieved for few-electron concentric double quantum rings (CDQR), experimentally realized a few years ago,[6] and we unveil a landscape of metastable localized states that appears at intermediate magnetic fields.

II. MODEL AND METHOD

The strictly two-dimensional CDQR are modeled by a circularly symmetric confining potential radially composed of two overlapping parabolas with frequencies ω_1 and ω_2, and vertices at radii R_1 and R_2 $(R_1<R_2)$, respectively:[7,8]

$$V_c(r)=\frac{m}{2}\min\{\omega_1^2(r-R_1)^2,\omega_2^2(r-R_2)^2\}. \tag{1}$$

The CDQR are submitted to a perpendicular magnetic field B pointing toward the positive z axis. Within the effective-mass approximation, the ground and excited N-electron states are obtained through the exact diagonalization of the Hamiltonian

$$\mathcal{H}=\sum_{i=1}^{N}\left[\frac{\left(\mathbf{p}_i+\frac{e}{c}\mathbf{A}_i\right)^2}{2m}+V_c(r_i)\right]+\sum_{i<j}^{N}\frac{e^2}{\epsilon|\mathbf{r}_i-\mathbf{r}_j|}+g^*\mu_B S_z B, \tag{2}$$

where $\mathbf{p}_i$, $\mathbf{r}_i$, and $\mathbf{A}_i=B/2(-y_i,x_i,0)$ are, respectively, the momentum, position, and vector potential operators acting upon the ith electron, $m=m^*m_e$ is the effective mass, where m_e is the bare electron mass, and μ_B is the Bohr magneton. S_z represents the z component of the total spin of the system, and in the present work always takes its maximum value, $N/2$, since the studied CDQR are submitted to high enough magnetic fields to be fully spin polarized. We impose this condition because we have previously found that CDQR present radial localization more easily in such fully polarized configurations,[8] and because it considerably simplifies the exact diagonalization procedure,[9,10] while it keeps the essential physics we aim to discuss. The rings are formed at a GaAs/AlGaAs heterostructure, characterized by an effective-mass ratio $m^*=0.067$, dielectric constant $\epsilon=12.4$, and effective gyromagnetic constant $g^*=-0.44$.

We have chosen two even electron numbers, $N=4$ and 6, which in a classical calculation for strictly one-dimensional concentric double rings (CDRs), where point-like electrons can only move at two fixed radii, display highly symmetric equilibrium states in which electrons are evenly distributed among both rings, yielding starred configurations of four and six points, as shown in Fig. 1. For the four-electron system we have taken $R_1=50$ nm, $R_2=70$ nm, $\omega_1=32$ meV, and $\omega_2=34$ meV, whereas for $N=6$ we have set $R_1=80$ nm, $R_2=100$ nm, $\omega_1=35$ meV, and $\omega_2=36.5$ meV.

For fixed N and B, the many-electron states $|\Psi_i^L\rangle$ corresponding to a given total angular momentum L in the negative z direction have been obtained within a configuration-interaction procedure, diagonalizing $\mathcal{H}$ in a basis of Slater determinants (SDs) built from Kohn-Sham single-particle (sp) states previously determined by solving the same CDQR

 ©2009 The American Physical Society

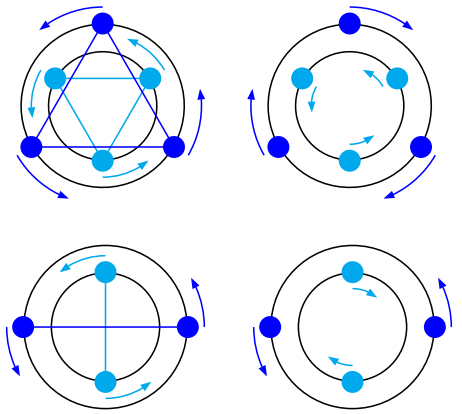

FIG. 1. (Color online) Diagrams of the classical starred configurations for one-dimensional CDR with $N=4$ and 6 point-like electrons. Rigid rotation (left column) and scissor modes (right column) are schematically displayed.

configuration within the local spin-density approximation (LSDA).[8] It has been shown[9,10] that this geometry-adapted basis improves the numerical procedure by reducing the number of SDs needed to accurately represent the relevant physical states. Figure 2 shows the energies of the lowest-lying spin-up sp states as a function of their angular momentum ℓ, for $N=4$ and $B=7.5$ T. They are distributed into "bands" corresponding to principal quantum numbers (number of radial nodes plus one) from $n=1$ to 4.

Diagonalizations have been performed by using the Lanczos algorithm implemented in the ARPACK package,[11] designed to address eigenvalue problems involving large sparse matrices. We have checked the accuracy of our results by reasonably increasing the number of SDs in the basis. For $N=4$, we have included all the sp states up to the minimum of the $n=4$, and even of the $n=5$ band. This is needed to address the high-energy part of the absorption spectrum in order to saturate the dipole sum rule (see below). However, we have checked that, in all cases up to $N=6$, it is enough to consider all the sp states up to the minimum of the $n=2$ band to accurately determine the ground-state energy.

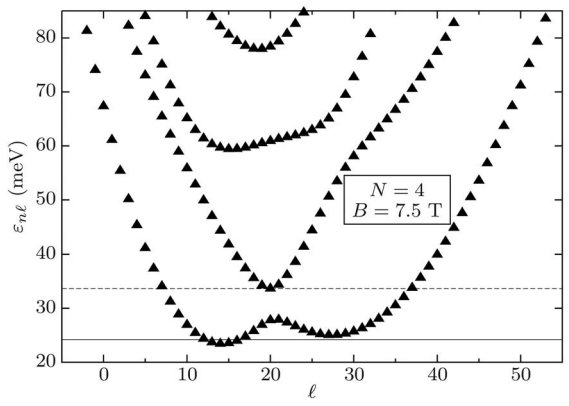

FIG. 2. Single-particle spin-up states for the CDQR with $N=4$ and $B=7.5$ T, obtained within the LSDA. The solid and dashed horizontal lines correspond, respectively, to the chemical potential and to the energy of the lowest state with $n=2$.

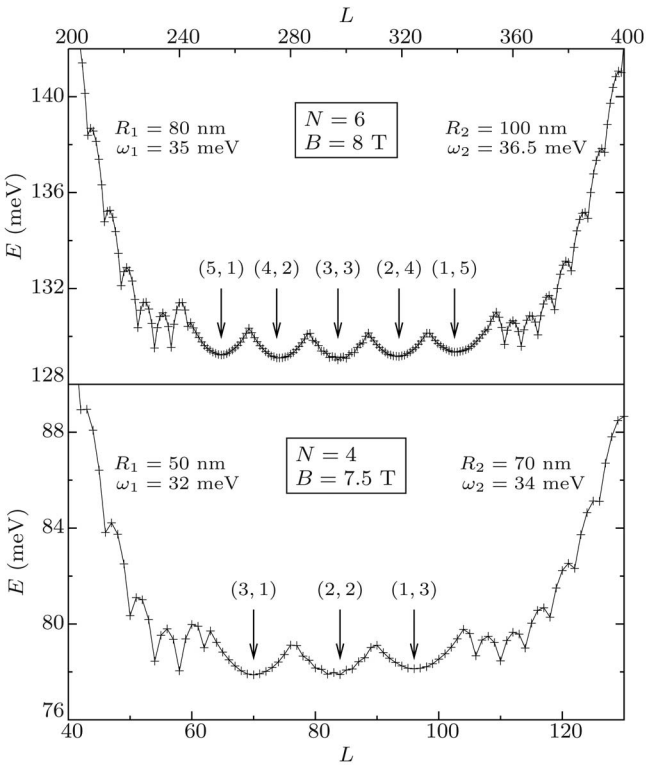

FIG. 3. Yrast line for the CDQR with $N=4$ at $B=7.5$ T (bottom panel), and for the CDQR with $N=6$ at $B=8$ T (top panel). For the $N=4$ ($N=6$) case, all sp states with energies up to the minimum of the $n=4$ ($n=2$) sp band have been used, yielding basis of up to 106 951 (133 037) SDs.

III. RESULTS AND DISCUSSION

Figure 3 shows the lowest total energy of the studied CDQR as a function of the total angular momentum, i.e., the yrast line $E(L)$,[12–14] for two selected geometries. At low (high) L values, the N electrons only occupy the inner (outer) ring, and we find in $E(L)$ the regularities of period N discussed in detail by Viefers *et al.*[14] in the case of noninteracting electrons, or of electrons classically interacting with several different interactions, occupying a single one-dimensional ring. In the noninteracting case, the N periodicity is easily understood since the lowest energy state for a given L is obtained by occupying N sp states of the first band as consecutively as possible, and completely compact states with strictly consecutive ℓ values can only be formed every N total angular momenta. This feature remains when the Coulomb interaction is incorporated.[15]

The yrast line displays another regularity, namely a series of $N-1$ quasiparabolic structures at intermediate values of L. This is a genuine CDQR effect that arises from this particular geometry, and is due to the progressive filling (emptying) of the outer (inner) ring as L increases. We call these structures *yrast traps*, in analogy to those displayed by nuclear systems.[12,16] Every one of the $N-1$ yrast traps displays a local minimum that corresponds, respectively, to the lowest energy state among those with $(N-i,i)$ electrons in the (inner, outer) ring. Each of these local-minimum many-electron states bears the intrinsic structure of a rigid rotator, as can be

seen, e.g., by comparison with the following simplified model:[1] if we write the energy of the quantized system corresponding to the classical $(N-i,i)$ configuration for the noninteracting one-dimensional CDR with rigidly disposed point-like electrons as

$$E_i(L) = \frac{\hbar^2 L^2}{2\mathcal{I}_i} - \frac{\hbar\omega_c}{2}L, \tag{3}$$

where $\mathcal{I}_i$ is the electronic moment of inertia of the i-th configuration and $\omega_c = eB/(mc)$ is the cyclotron frequency, minimizing this expression with respect to L yields for the positions of the local minima $L_{0,i} = \mathcal{I}_i\omega_c/(2\hbar)$, which are linear in the magnetic field intensity. Within this model, local parabolic minima are predicted at $L_0 = 71, 84$, and 98 for $N=4$ and $B=7.5$ T, and at $L_0 = 255$, 277, 299, 321, and 343 for $N=6$ and $B=8$ T, in very good agreement with the values displayed along the yrast line (see Fig. 3). These minimum-energy states are the CDQR realization of the well-known isomeric states in nuclear physics,[12,17] namely metastable states close enough in energy to the ground state but with fairly different values of the angular momentum, which makes them very long lived as they cannot easily decay by electromagnetic radiation, e.g., dipole emission in the present case. Depending on the charge process of the CDQR, one may populate any of these long-lived states.

Two final considerations, in agreement with the simple rotator model, should be made concerning the yrast structure for intermediate L values: First, yrast traps are formed even for noninteracting electrons, and the main effect of the Coulomb interaction on them is the change in the relative energies of the different traps. Second, the sequence of traps behaves robustly when varying B: the ΔL's between isomeric states increase linearly with the magnetic field, as well as the energy barriers between the traps; this implies that the effect vanishes in the limit of low magnetic fields, in agreement with previous studies.[7,8]

While the one-body electron density of the system is always circularly symmetric, this is not the case for the two-body density

$$\rho^{(2)}(\mathbf{r}_1,\mathbf{r}_2) = \langle\Psi|\sum_{i\neq j}\delta(\mathbf{r}_i' - \mathbf{r}_1)\delta(\mathbf{r}_j' - \mathbf{r}_2)|\Psi\rangle \tag{4}$$

of localized many-electron configurations.[1–3] This is illustrated in Fig. 4, where we show $\rho^{(2)}(\mathbf{r}_1,\mathbf{r}_2)$ for $N=4$, $L_0=84$, and $B=7.5$ T, and for $N=6$, $L_0=297$, and $B=8$ T. These configurations correspond to the classical four- and six-point starred ones represented in Fig. 1.

Finally, we discuss an observable signature of the localized molecular states. We have computed the dipole strength function that characterizes the infrared absorption[18]

$$S(\omega) = \sum_{L=L_0\pm1}\sum_k |\langle\Psi_k^L|D|\Psi_0^{L_0}\rangle|^2\delta(\omega - \omega_{k0}^{(L)}), \tag{5}$$

where $|\Psi_0^{L_0}\rangle$ is either the ground or an isomeric state of the CDQR with angular momentum L_0, which is connected to the excited states $|\Psi_k^{L_0\pm1}\rangle$ with angular momenta $L_0\pm1$ through the dipolar operator $D=\Sigma_{j=1}^N x_j$, and $\omega_{k0}^{(L)}$ is the energy difference between $|\Psi_k^L\rangle$ and $|\Psi_0^{L_0}\rangle$.

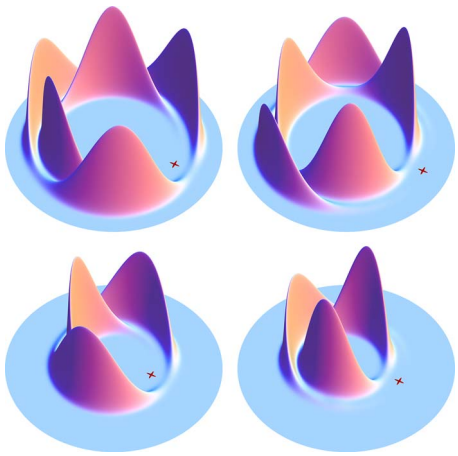

FIG. 4. (Color online) Two-body density for $N=4$, $L_0=84$, and $B=7.5$ T (bottom row), and for $N=6$, $L_0=297$, and $B=8$ T (top row), when one electron (cross) is located in the inner ring (left column) or in the outer ring (right column).

Figure 5 shows the low-energy absorption spectrum for $N=4$, $B=7.5$ T, and $L_0=70$, and for $N=6$, $B=8$ T, and $L_0=275$. In the case of $N=4$, the inset shows the dipole spectrum for energies below ~43 meV. To obtain it, we have included in Eq. (5) 4000 many-electron states to have access to the high-energy transitions involving $\Delta n=2$ sp components in Fig. 2. We have checked that, in this case, a 97% of the Thomas-Reiche-Kuhn sum rule[18] is exhausted, the remaining 3% being associated to higher energy excitations. Figure 5 shows that, besides dipole excitations that can be easily associated with edge modes in either ring and with bulk-like excitations,[19] a very soft mode appears whose en-

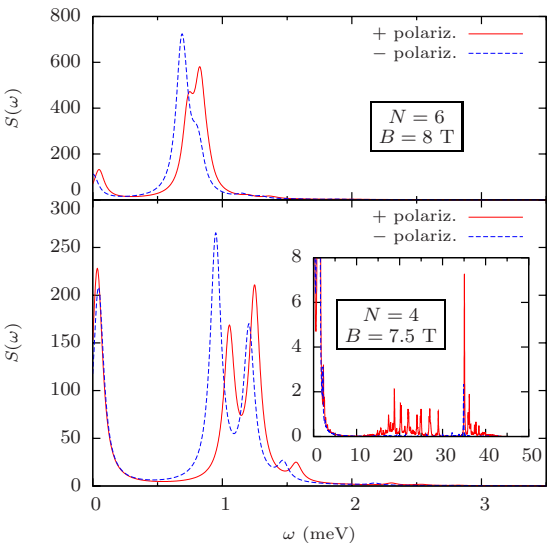

FIG. 5. (Color online) Low-energy dipole absorption spectrum, in arbitrary units, for the $N=4$, $L_0=70$ CDQR at $B=7.5$ T (botom panel), and for the $N=6$, $L_0=275$ CDQR at $B=8$ T (top panel). The inset in the bottom panel displays the dipole spectrum corresponding to the lowest energy 4000 excitations for each polarization. Solid lines correspond to the (+) circular polarization, and dashed lines to the (−) circular polarization. Peaks are represented by Lorentzians of 0.1 meV full width at half maximum.

ergy is similar to the one obtained from Eq. (3) for the dipolar absorption on the underneath classical molecular configuration when $L_{0,i} \rightarrow L_{0,i} \pm 1$, $\Delta E_i = \hbar^2/(2\mathcal{I}_i)$. In particular, the energies of the classical modes for the configurations corresponding to the states in Fig. 5 are 4.6×10^{-2} meV for $N=4$, and 1.2×10^{-2} meV for $N=6$. We have computed $S(\omega)$ for the other isomeric states displayed in Fig. 3, and have also found a soft mode for them. The relative intensities of these modes depend on the "rigidity" of the electronic configuration, the more rigid the isomeric state, the more intense the peak.

It is worthwhile pointing out that, besides the rotational mode corresponding to a rigid angular displacement of all the electrons in the one-dimensional CDQR, there are other classical modes, vibrational ones, that correspond to internal displacements of some electrons with respect to others, and that do not appear in the dipole spectra. Among these excitations, the most interesting one is the *scissor* mode,[18] where the electrons of one ring rigidly rotate clockwise, whereas the electrons of the other ring rigidly rotate counterclockwise, as displayed in Fig. 1. Scissor modes have already been found in deformed atomic nuclei[20] and Bose-Einstein condensates,[21] and should appear in the quadrupole absorption spectrum as the rigid rotator does in the dipole one, reinforcing the molecular many-electron states picture.

IV. CONCLUSION

We have shown that CDQR host isomeric many-electron states whose internal structure displays radial and azimuthal electronic localization in either constituent ring. The absorption spectra of these states show very soft modes whose energy qualitatively agrees with the dipole excitation of the underneath rigid rotator, and which might be observed by far-infrared spectroscopy. Other classical excitation modes, such as the scissor mode, likely have a quantum analog that should show up in the quadrupole response, whose study is currently under way.

ACKNOWLEDGMENTS

The authors thank M. Barranco, Ll. Serra, and E. Lipparini for useful discussions. This work has been performed under Grant No. FIS2008-00421 from DGI (Spain).

[1] P. A. Maksym, H. Imamura, G. P. Mallon, and H. Aoki, J. Phys.: Condens. Matter **12**, R299 (2000).
[2] S. M. Reimann and M. Manninen, Rev. Mod. Phys. **74**, 1283 (2002).
[3] C. Yannouleas and U. Landman, Rep. Prog. Phys. **70**, 2067 (2007).
[4] A. Puente, Ll. Serra, and R. G. Nazmitdinov, Phys. Rev. B **69**, 125315 (2004); A. Ghosal, A. D. Guclu, C. J. Umrigar, D. Ullmo, and H. U. Baranger, Nat. Phys. **2**, 336(L) (2006); S. Kalliakos, M. Rontani, V. Pellegrini, C. P. García, A. Pinczuk, G. Goldoni, E. Molinari, L. N. Pfeiffer, and K. W. West, *ibid.* **4**, 467(L) (2008).
[5] L. Wendler, V. M. Fomin, A. V. Chaplik, and A. O. Govorov, Phys. Rev. B **54**, 4794 (1996); M. Koskinen, M. Manninen, B. Mottelson, and S. M. Reimann, *ibid.* **63**, 205323 (2001); F. Pederiva, A. Emperador, and E. Lipparini, *ibid.* **66**, 165314 (2002); A. Emperador, F. Pederiva, and E. Lipparini, *ibid.* **68**, 115312 (2003).
[6] T. Mano, T. Kuroda, S. Sanguinetti, T. Ochiai, T. Tateno, J. Kim, T. Noda, M. Kawabe, K. Sakoda, G. Kido, and N. Koguchi, Nano Lett. **5**, 425 (2005); T. Kuroda, T. Mano, T. Ochiai, S. Sanguinetti, K. Sakoda, G. Kido, and N. Koguchi, Phys. Rev. B **72**, 205301 (2005); A. Mühle, W. Wegscheider, and R. J. Haug, Appl. Phys. Lett. **91**, 133116 (2007); S. Bietti, C. Somaschini, M. Abbarchi, N. Koguchi, S. Sanguinetti, E. Poliani, M. Bonfanti, M. Gurioli, A. Vinattieri, T. Kuroda, T. Mano, and S. Sakoda, Phys. Status Solidi C **6**, 928 (2009).
[7] B. Szafran and F. M. Peeters, Phys. Rev. B **72**, 155316 (2005).
[8] F. Malet, E. Lipparini, M. Barranco, and M. Pi, Phys. Rev. B **73**, 125302 (2006); L. Colletti, F. Malet, M. Pi, and F. Pederiva, *ibid.* **79**, 125315 (2009).
[9] A. Emperador, E. Lipparini, and F. Pederiva, Phys. Rev. B **72**, 033306 (2005).
[10] M. Rontani, C. Cavazzoni, D. Bellucci, and G. Goldoni, J. Chem. Phys. **124**, 124102 (2006).
[11] R. B. Lehoucq, K. Maschhoff, D. C. Sorensen, and C. Yang, ARPACK computer code, 1997 (http://www.caam.rice.edu/software/ARPACK/).
[12] A. Bohr and B. R. Mottelson, *Nuclear Structure* (W. A. Benjamin, New York, 1975), Vol. 2; P. Ring and P. Schuck, *The Nuclear Many-Body Problem* (Springer-Verlag, New York, 1980).
[13] B. Mottelson, Phys. Rev. Lett. **83**, 2695 (1999).
[14] S. Viefers, P. Koskinen, P. Singha Deo, and M. Manninen, Physica E **21**, 1 (2004).
[15] T. Chakraborty and P. Pietiläinen, Phys. Rev. B **50**, 8460 (1994).
[16] A. Faessler, M. Ploszajczak, and K. R. S. Devi, Phys. Rev. Lett. **36**, 1028 (1976).
[17] Nuclear isomeric states are yrast metastable states which cannot undergo a rapid γ-transition.
[18] E. Lipparini, *Modern Many-Particle Physics: atomic gases, nanostructures and quantum liquids* (World Scientific, Singapore, 2008).
[19] C. Dahl, J. P. Kotthaus, H. Nickel, and W. Schlapp, Phys. Rev. B **48**, 15480 (1993); A. Lorke and R. J. Luyken, Physica B **256-258**, 424 (1998); A. Emperador, M. Pi, M. Barranco, and A. Lorke, Phys. Rev. B **62**, 4573 (2000).
[20] N. Lo Iudice and F. Palumbo, Phys. Rev. Lett. **41**, 1532 (1978); D. Bohle, A. Richter, W. Steffen, A. E. L. Dieperink, N. Lo Iudice, F. Palumbo, and O. Scholten, Phys. Lett. B **137**, 27 (1984).
[21] M. Cozzini, S. Stringari, V. Bretin, P. Rosenbusch, and J. Dalibard, Phys. Rev. A **67**, 021602(R) (2003).